

Analysis of transmission line feed method for transparent conductor oxide materials based optical microstrip patch antennas design

AHMED NABIH ZAKI RASHED*, HAMDY A. SHARSHAR

Electronics and Electrical Communications Engineering Department Faculty of Electronic Engineering, Menouf 32951, Menoufia University, Egypt

This paper has presented transparent conductor oxide materials (TCOMs) based microstrip patch antennas with glass substrate and copper ground plane which have been deeply analyzed in the visible spectrum region in comparison with practical patch antenna model of indium tin oxide patch with glass substrate and different TCOMs based ground plane. As well as the study will analyze the effect of transparent oxide materials on patch antenna design instead of perfect conductor materials such as copper to be low cost and weight. The tradeoff between optical transparency and electrical conductivity will be evaluated for a range of visible regions. Microstrip transmission line feed method is used to predict the skin effects on a patch antenna and their impact on antenna efficiency, resonance frequency and optical transmission are also described. The assessment of these tradeoffs and effect of TCOMs parameters for antenna design.

(Received July 9, 2012; accepted October 30, 2012)

Keywords: Transparent conductor materials, Transmission line feed method, Antenna efficiency, Visible region

1. Introduction

Microstrip antennas are attractive due to their light weight, conformability and low cost. These antennas can be integrated with printed strip line feed networks and active devices [1]. This is a relatively new area of antenna engineering. Rectangular and circular micro strip resonant patches have been used extensively in a variety of array configurations. A major contributing factor for recent advances of microstrip antennas is the current revolution in electronic circuit miniaturization brought about by developments in large scale integration. As conventional antennas are often bulky and costly part of an electronic system, micro strip antennas based on photolithographic technology are seen as an engineering breakthrough [2]. A microstrip antenna consists of conducting patch on a ground plane separated by dielectric substrate. After that many authors have described the radiation from the ground plane by a dielectric substrate for different configurations [3]. The micro strip antennas are the present day antenna designer's choice. Low dielectric constant substrates are generally preferred for maximum radiation. The conducting patch can take any shape but rectangular and circular configurations are the most commonly used configuration. Other configurations are complex to analyze and require heavy numerical computations. A microstrip antenna is characterized by its length, width, input impedance, and gain and radiation patterns [4]. Various parameters of the microstrip antenna and its design considerations will be discussed in the subsequent sections. The length of the antenna is nearly half wavelength in the dielectric; it is a very critical parameter, which governs the resonant frequency of the antenna.

There are no hard and fast rules to find the width of the patch [5].

Transparent conductive materials have been prepared with oxides of tin, indium, zinc and cadmium [6]. These transparent conducting oxides (TCOs) are employed in a wide spectrum of applications such as solar cells, electromagnetic shielding and touch-panel controls [7]. Notably, there has been little commercial application of TCOs in antenna design. Attempts have been made to create transparent patch antennas for automobile windshields and solar cells. Many researchers on this subject express the inability to achieve high gains (> 2 dB) [8] and reduced efficiencies of microstrip antennas compared to antennas that are not near a ground plane, such as a dipole in free space. Previous transparent antenna research offers little insight into the use and limitations of TCO antennas in general, and what range of conductivity and transparency can be expected from today's materials and how that impacts antenna performance for different frequency bands [9]. This study have deeply investigated the effect of antenna dimensions such as patch length (L), width (W), patch thickness (t) and substrate parameters relative to dielectric substrate constant (ϵ_r) and substrate height (h) on the radiation parameters of bandwidth radiation efficiency, radiation resistance and optical transmission coefficient.

2. Microstrip patch antenna basic structure

In its most fundamental form, a microstrip patch antenna consists of a radiating patch on one side of a dielectric substrate which has a ground plane on the other

side as shown in Fig. 1. The patch is generally made of transparent conducting oxide materials (TCOMs) such as indium tin oxide (ITO), antimony tin oxide (ATO), titanium indium oxide (TIO), and gallium zinc oxide (GZO) and can take any possible shape. The radiating patch and the feed lines are usually photo etched on the dielectric substrate [9].

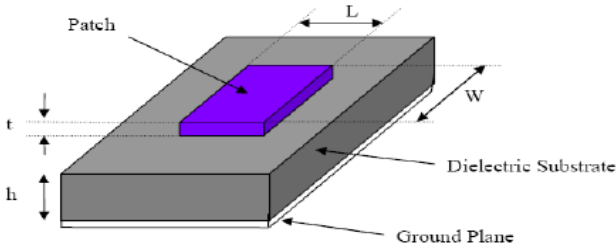


Fig. 1. Schematic view of microstrip patch antenna.

In order to simplify analysis and performance prediction, the patch is generally square, rectangular, circular, triangular, and elliptical or some other common shapes. For a rectangular patch configuration, the length of the patch L , patch thickness t and the height of the dielectric substrate h . The dielectric constant of the glass substrate ($\epsilon_{r(\text{Glass})}=6$) and the ground plane is copper and is considered to be a perfect electric conductor (PEC) with $\epsilon_{r(\text{Cu})}=1.002$, $N_{e(\text{Cu})}=846 \times 10^{26} \text{ m}^{-3}$, and $\mu_{e(\text{Cu})}=440 \text{ cm}^2 \text{ V}^{-1} \text{ s}^{-1}$. Microstrip patch antennas radiate primarily because of the fringing fields between the patch edge and the ground plane, thus $(\epsilon_r = \epsilon_{\text{TCM}} + \epsilon_{r(\text{Glass})} + \epsilon_{r(\text{Cu})})$ [10]. For good antenna performance, a thick dielectric substrate having a low dielectric constant is desirable since this provides better efficiency, larger bandwidth and better radiation. However, such a configuration leads to a larger antenna size. In order to design a compact Microstrip patch antenna, substrates with higher dielectric constants must be used which are less efficient and result in narrower bandwidth. Hence a trade off must be realized between the antenna dimensions and antenna performance [11].

3. Transmission line method analysis

This model represents the microstrip antenna by two slots of width W and height h , separated by a transmission line of length L . The microstrip is essentially a non homogeneous line of two dielectrics, typically the substrate and air. Consider Fig. 2 below, which shows a rectangular microstrip patch antenna of length L , width W resting on a substrate of height h . The co-ordinate axis is selected such that the length is along the x direction, width is along the y direction and the height is along the z direction [12].

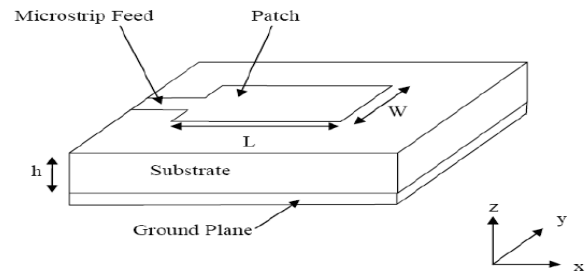


Fig. 2. Rectangular microstrip patch antenna.

In order to operate in the fundamental TM_{10} mode, the length of the patch must be slightly less than $\lambda/2$ where λ is the wavelength in the dielectric medium and is equal to $\lambda_{\text{visible}} / (\epsilon_{\text{reff}})^{0.5}$, where λ_{visible} is the free space visible wavelength. The TM_{10} mode implies that the field varies one $\lambda/2$ cycle along the length, and there is no variation along the width of the patch.

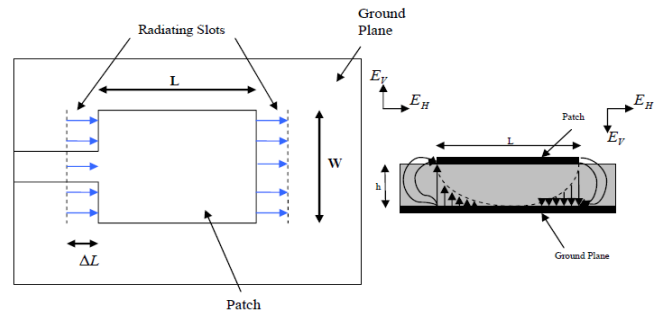


Fig. 3. Top and side views of the antenna.

In the Fig. 3 shown above, the microstrip patch antenna is represented by two slots, separated by a transmission line of length L and open circuited at both the ends. Along the width of the patch, the voltage is maximum and current is minimum due to the open ends. The fields at the edges can be resolved into normal and tangential components with respect to the ground plane [13]. It is seen from Fig. 3 that the normal components of the electric field at the two edges along the width are in opposite directions and thus out of phase since the patch is $\lambda/2$ long and hence they cancel each other in the broadside direction. The tangential components (seen in Fig. 3), which are in phase, means that the resulting fields combine to give maximum radiated field normal to the surface of the structure. Hence the edges along the width can be represented as two radiating slots, which are $\lambda/2$ apart and excited in phase and radiating in the half space above the ground plane [14].

4. Antenna model analysis

An effective dielectric constant (ϵ_{reff}) must be obtained in order to account for the fringing and the wave propagation in the line. The value of ϵ_{reff} is slightly less

then ϵ_r because the fringing fields around the periphery of the patch are not confined in the dielectric substrate but are also spread in the air. The expression for ϵ_{reff} is given by [15]:

$$\epsilon_{\text{reff}} = \frac{\epsilon_r + 1}{2} + \frac{\epsilon_r - 1}{2} \left(1 + 12 \frac{h}{W} \right)^{0.5}, \quad (1)$$

Where W is the patch width, ϵ_r is the dielectric substrate constant, and h is the substrate height. The fringing fields along the width can be modeled as radiating slots and electrically the patch of the microstrip antenna looks greater than its physical dimensions. The dimensions of the patch along its length have now been extended on each end by a distance ΔL , which is given empirically by [16] as:

$$\Delta L = 0.412h \frac{(\epsilon_{\text{reff}} + 0.3) \left(\frac{W}{h} + 0.264 \right)}{(\epsilon_{\text{reff}} - 0.258) \left(\frac{W}{h} - 0.8 \right)}, \quad (2)$$

The effective length of the microstrip patch antenna L_{eff} now becomes:

$$L_{\text{eff}} = L + 2\Delta L, \quad (3)$$

For a rectangular microstrip patch antenna, the resonance frequency for the fundamental TM_{10} mode is given by [17]:

$$f_0 = \frac{c}{2L_{\text{eff}} \sqrt{\epsilon_{\text{reff}}}}, \quad (4)$$

for efficient radiation, the effective width of the microstrip patch antenna W_{eff} can be expressed as [18]:

$$W_{\text{eff}} = \frac{c}{2f_0 \sqrt{\frac{\epsilon_r + 1}{2}}}, \quad (5)$$

Where c is the speed of light (3×10^8 m/sec). The electron mobility, density and permittivity, of various are listed as shown in Table 1. Where m_e is the electron mass (9.1×10^{-31} kg).

Table 1. Electron mobility, permittivity, effective electron mass and density of various TCOMs.

Transparent conductor material (TCM)	Mobility μ_e ($\text{cm}^2 \text{V}^{-1} \text{s}^{-1}$)	Density N_e (m^{-3})	Effective electron mass m^*	Permittivity ϵ_{TCM}
ITO [13]	45	4×10^{26}	$0.35 m_e$	4
ATO [10]	9.7	1.26×10^{26}	$0.11 m_e$	1.26
TiO [22]	80	8×10^{26}	$0.7 m_e$	8
GZO [20]	13	1×10^{26}	$0.0875 m_e$	1.1

The conductivity of TCOMs as a function of effective visible wavelength can be expressed as [19]:

$$|\sigma| = \frac{(N_{e(\text{TCM})} + N_{e(\text{Cu})}) q (\mu_{e(\text{TCM})} + \mu_{e(\text{Cu})}) \lambda_{\text{Visible}}}{\sqrt{\lambda_{\text{Visible}}^2 + 4\pi^2 c^2 \tau^2}}, \quad (6)$$

Where $N_{e(\text{TCM})}$ is the electron density for transparent conductor material, $N_{e(\text{Cu})}$ is the electron density for copper conductor perfect material, q is the electron charge, $\mu_{e(\text{TCM})}$ is the electron mobility for transparent conductor material, $\mu_{e(\text{Cu})}$ is the electron mobility for copper perfect conductor material and τ is the electronic relaxation time which is defined by the following formula:

$$\tau = \frac{m^* (\mu_{e(\text{TCM})} + \mu_{e(\text{Cu})})}{q}, \quad (7)$$

Where m^* is the effective electron mass. The transmission of light through a TCOMs are well approximated by [20]:

$$T \approx \exp\left(-\frac{t}{2\delta}\right), \quad (8)$$

Where t is the microstrip patch antenna thickness, and δ is the skin depth which is given by [21]:

$$\delta = \frac{8\pi^2 m^{*2} c^2 (\mu_{e(\text{TCM})} + \mu_{e(\text{Cu})})}{Z_{\text{TCM}} q^3 \lambda_{\text{Visible}}^2 (N_{e(\text{TCM})} + N_{e(\text{Cu})})}, \quad (9)$$

Where $Z_{\text{TCM}} = 377 / (\epsilon_{\text{TCM}})^{0.5}$ in Ω . According to the assumption $W/h \gg 1$, in this case, the surface resistance can be defined as [22-24]:

$$R_s \approx \frac{2L}{|\sigma| \delta W \left(1 - e^{-\frac{0.5t}{\delta}} \right)}, \quad (10)$$

The rectangular microstrip patch antennas were designed with input impedance $R_A = 50$. Therefore the radiation efficiency in this case is calculated as [25]:

$$\eta_r = \frac{R_A}{R_A + R_s}, \quad (11)$$

5. Simulation results and performance evaluation

Optical antennas have been deeply investigated for microstrip patch antennas in the visible spectrum region to enhance its performance operation characteristics such as antenna gain, optical transmission, skin depth losses and antenna efficiency over wide range of the affecting operating parameters as shown in Table 2.

Table 2. Operating parameters for optical microstrip patch antennas [13, 15, 20, 22, 25].

Operating parameter	Symbol	Value
Operating optical signal wavelength (Visible region)	λ_{Visible}	$400 \leq \lambda_{\text{Visible}}, \text{ nm} \leq 700$
Patch length	L	50 μm
Patch width	W	30 μm
Patch thickness	t	0.1 μm -2.5 μm
Glass substrate dielectric constant	$\epsilon_{r(\text{Glass})}$	6
Dielectric substrate height	h	5 μm -20 μm
Electron charge	q	$1.6 \times 10^{-19} \text{ C}$

Based on the modeling equations analysis over wide range of the operating parameters, and the series of the Figs. (4-12), the following features are assured:

- i) Figs. (4-6) have assured that optical transmission coefficient decreases with increasing both operating optical signal wavelength in the visible region and antenna patch thickness for different antenna patch structures. It is theoretically found that TIO based patch antenna has presented the highest optical

transmission coefficient compared to other materials under the same operating conditions.

- ii) As shown in Figs. (7-9) have indicated that antenna radiation efficiency increases with increasing patch thickness and decreasing operating optical signal wavelength in the visible region. It is observed that TIO based patch antenna has presented the highest radiation efficiency compared to other materials under the same operating considerations.

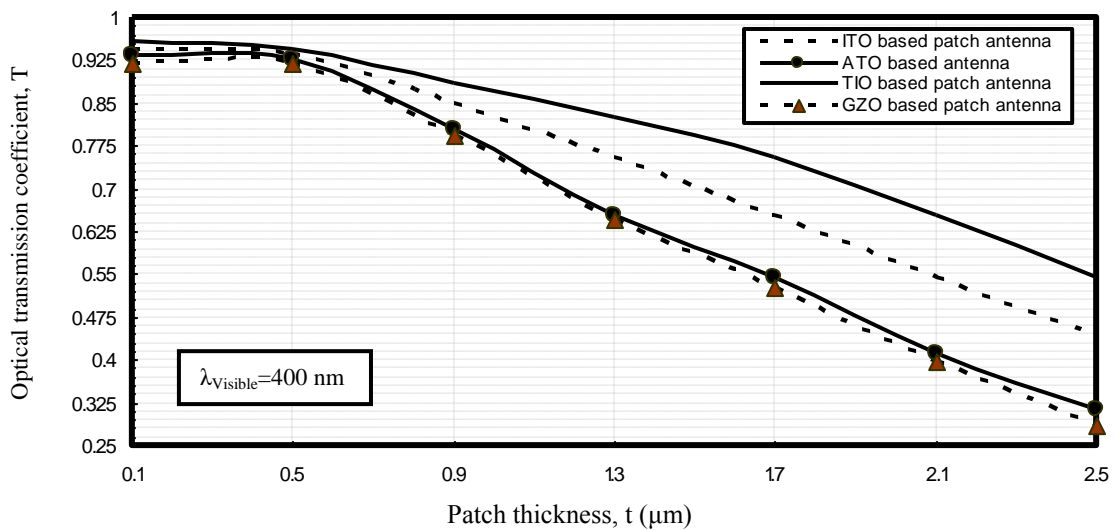


Fig. 4. Optical transmission coefficient in relation to patch antenna thickness and visible wavelength for various transparent conductor oxide materials based patch antenna at the assumed set of the operating parameters.

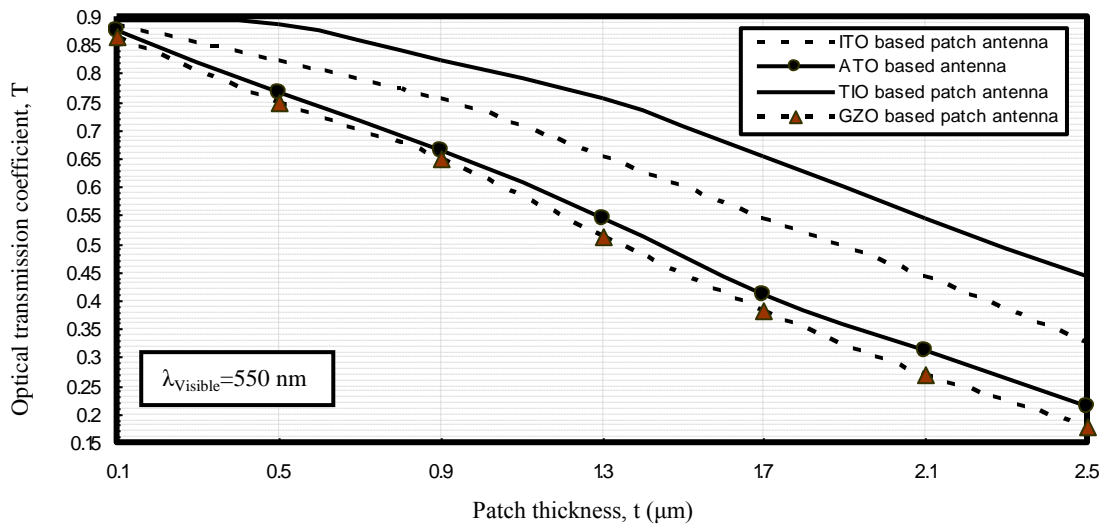


Fig. 5. Optical transmission coefficient in relation to patch antenna thickness and visible wavelength for various Transparent conductor oxide materials based patch antenna at the assumed set of the operating parameters.

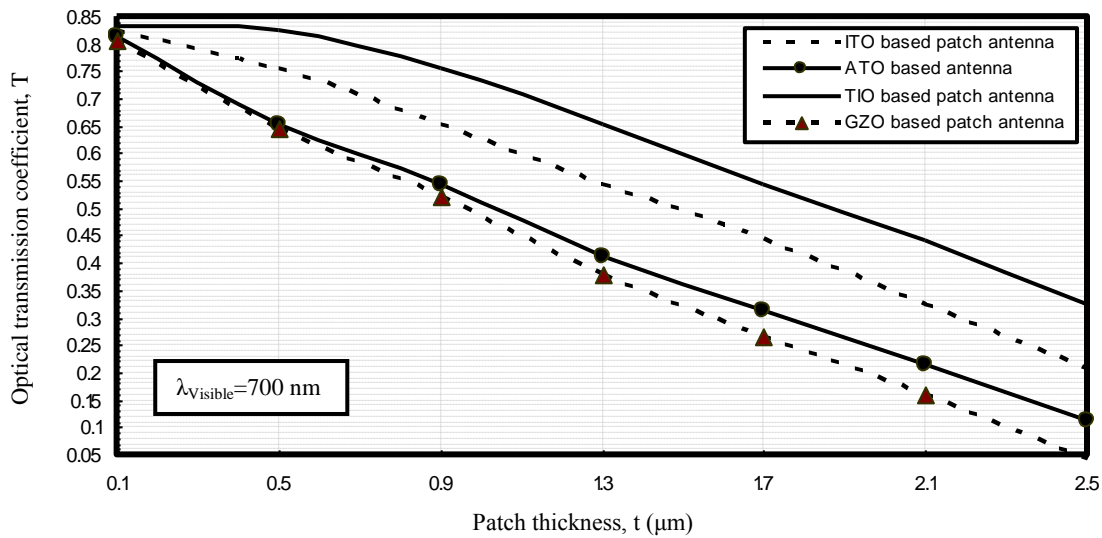


Fig. 6. Optical transmission coefficient in relation to patch antenna thickness and visible wavelength for various transparent conductor oxide materials based patch antenna at the assumed set of the operating parameters.

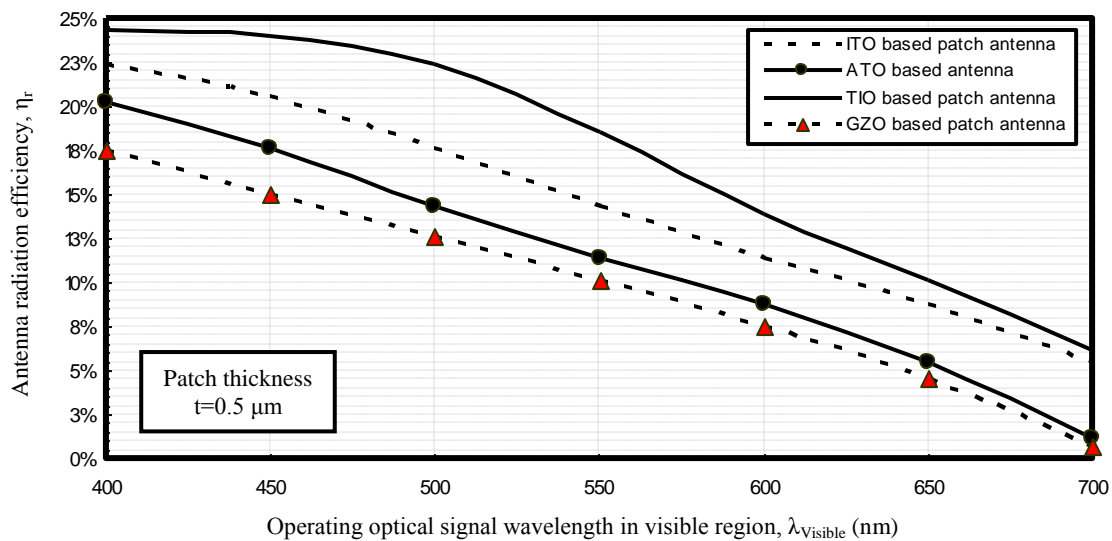


Fig. 7. Antenna radiation efficiency in relation to visible optical wavelength and patch antenna thickness for various transparent conductor oxide materials based patch antenna at the assumed set of the operating parameters.

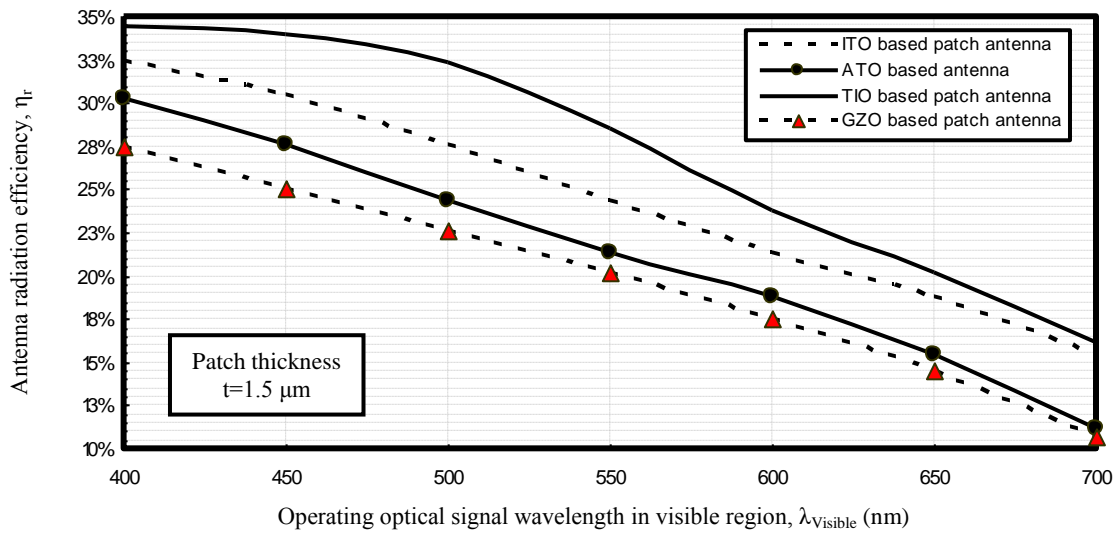


Fig. 8. Antenna radiation efficiency in relation to visible optical wavelength and patch antenna thickness for various transparent conductor oxide materials based patch antenna at the assumed set of the operating parameters.

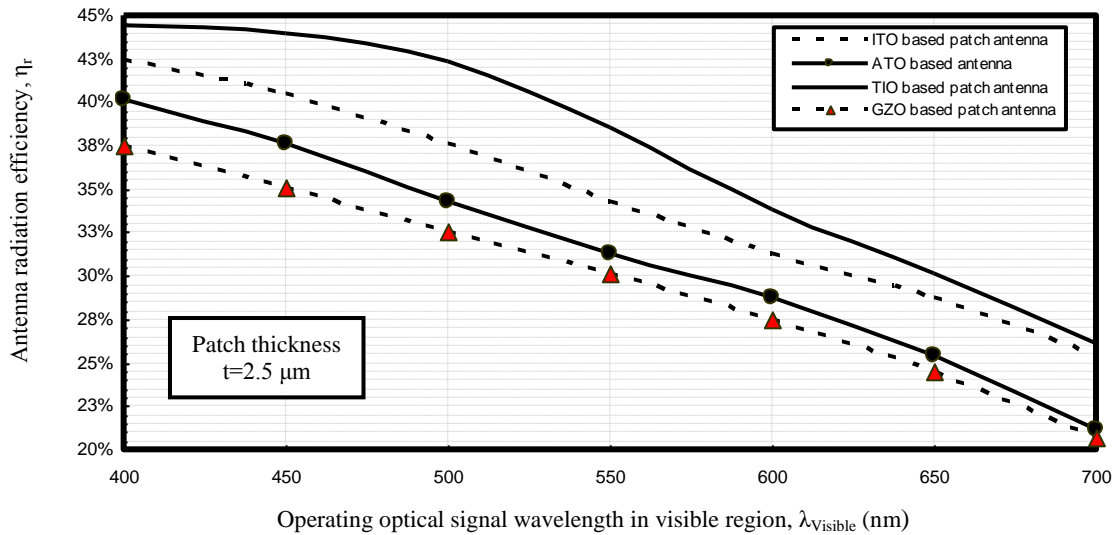


Fig. 9. Antenna radiation efficiency in relation to visible optical wavelength and patch antenna thickness for various transparent conductor oxide materials based patch antenna at the assumed set of the operating parameters.

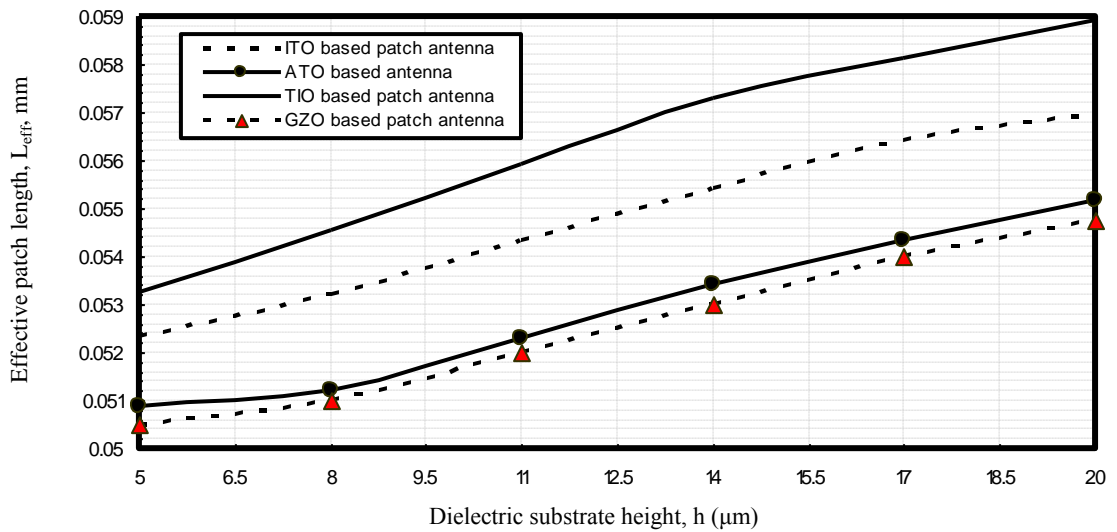


Fig. 10. Effective patch length in relation to dielectric substrate height for various transparent conductor oxide materials based patch antenna at the assumed set of the operating parameters.

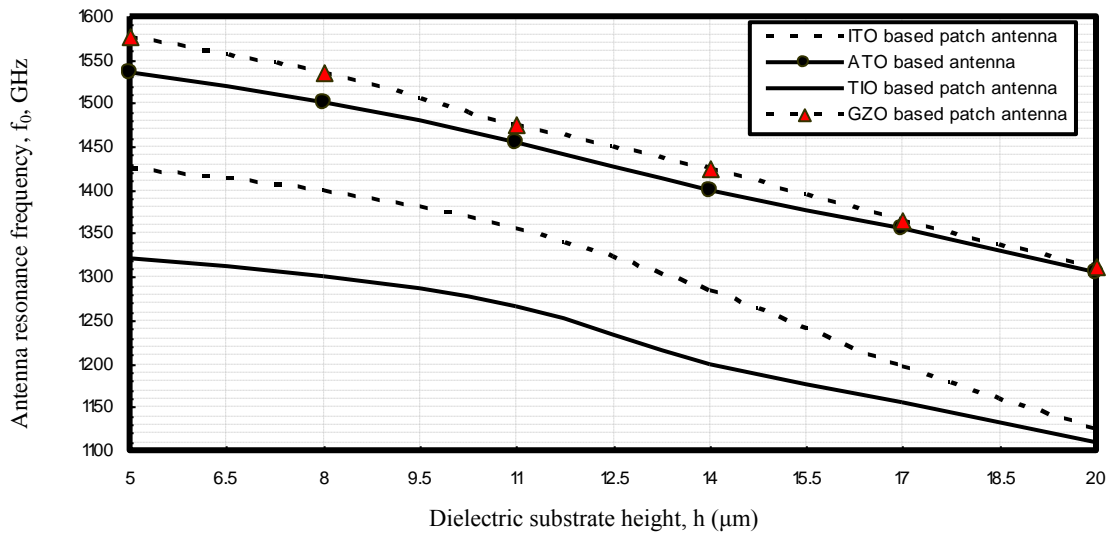


Fig. 11. Antenna resonance frequency in relation to dielectric substrate height for various transparent conductor oxide materials based patch antenna at the assumed set of the operating parameters.

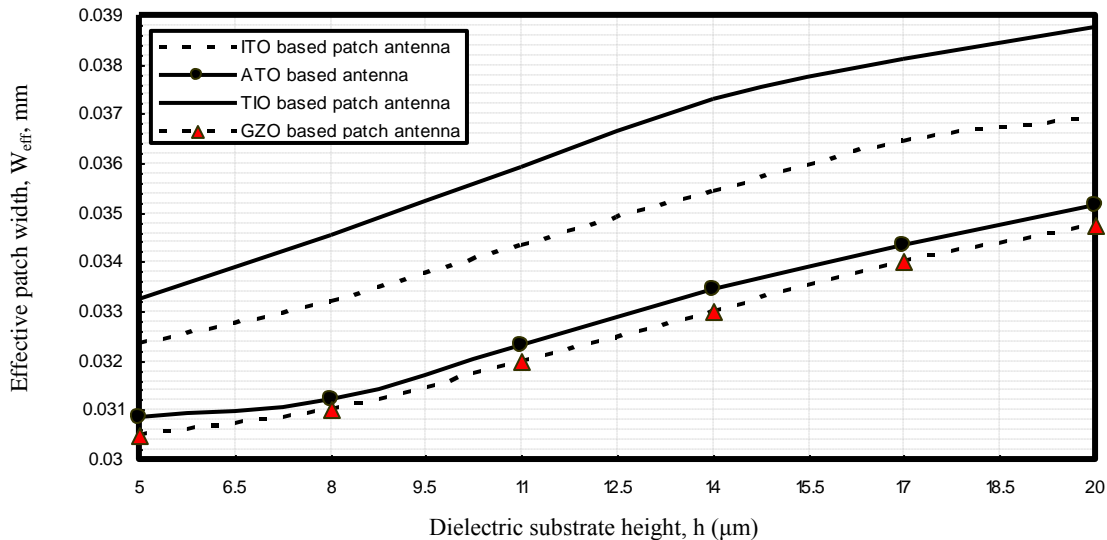


Fig. 12. Effective patch width in relation to dielectric substrate height for various transparent conductor oxide materials based patch antenna at the assumed set of the operating parameters.

- iii) Figs. (10-12) have demonstrated that effective antenna length and width increase with increasing antenna dielectric substrate height, while antenna resonance frequency decreases with increasing its dielectric substrate height. As well as TIO based patch antenna has presented the highest effective length and width and the lowest resonance frequency compared to other materials under the same operating conditions.

6. Conclusions

These transparent antennas have very poor radiation efficiencies at wavelengths at 700 nm. Fair efficiencies (more than 40%) are achieved for wavelength at 400 nm with thick thickness. It is theoretically found that electron mobility above $\mu_e = 100 \text{ cm}^2\text{V}^{-1}\text{s}^{-1}$ is very hard to achieve and further materials development should be done to

improve the electron mobility of TCOMs, novel materials such as titanium doped indium oxide could provide higher than $\mu_e = 50 \text{ cm}^2\text{V}^{-1}\text{s}^{-1}$ mobility. It is indicated that if the ground plane is fabricated of copper material, the radiation efficiency is improved to reach 44.5 % at $\lambda_{\text{visible}} = 400 \text{ nm}$, and patch thickness $t = 2.5 \text{ μm}$ because the ground and skin depth effects are minimal for these transparent antennas due to copper's high free electron density ($N_e = 846 \times 10^{26} \text{ m}^{-3}$) and electron mobility of ($\mu_e = 440 \text{ cm}^2\text{V}^{-1}\text{s}^{-1}$). Theoretical results has presented high both optical transmission coefficient and radiation efficiency if these transparent material is coupled with ground plane made of copper material. While it is observed that if the ground plane is also transparent, the radiation efficiency η_r would drop substantially due to ground surface resistance R_s , so mobility would become even more critical according to our theoretical results in comparison with practical results as summarized in Table 3.

Table 3. Comparison our theoretical design parameters of optical microstrip patch antennas with practical results.

Design Parameters	Our theoretical results				Practical results [22, 24, 26, 27]		
	Our Antenna structures				Their Antenna structures		
	Antenna structure consists of both fixed glass substrate, and copper ground plane with different antenna patches at the same operating conditions: $h=5 \mu\text{m}$, $t=2.5 \mu\text{m}$, and $\lambda_{\text{visible}}=400 \text{ nm}$.				Antenna structure consists of fixed both glass substrate and ITO patch antenna with different ground planes at the same operating conditions: $h=5 \mu\text{m}$, $t=2.5 \mu\text{m}$, and $\lambda_{\text{visible}}=400 \text{ nm}$.		
	Patch (1)	Patch (2)	Patch (3)	Patch (4)	Plane (1)	Plane (2)	Plane (3)
	ITO	ATO	TIO	GZO	ATO	TIO	GZO
Optical transmission (T)	0.475	0.325	0.55	0.31	0.258	0.432	0.277
Radiation efficiency (η_r)	43%	40%	44.5%	38%	28.5%	33.7%	21.32%
Resonance frequency (f_0), GHz	1425	1545	1325	1575	80	54	100
Effective length (L_{eff}), mm	0.0525	0.051	0.0535	0.0505	10.25	18.75	9.35
Effective width (W_{eff}), mm	0.0324	0.03	0.0332	0.0304	7.3	12.65	6.75

References

- [1] Randy Bancroft, Second Edition, SciTech Publishing, 2009.
- [2] John L. Volakis, McGraw-Hill, 2007.
- [3] K. L. Wong, Compact and Broadband Microstrip Antennas. New York, NY: John Wiley and Sons Inc., 2002.
- [4] Reena Pant, Pradyot Kala1, S. S. Pattnaik, R. C. Saraswat, International Journal of Microwave and Optical Technology, 443 (2008).
- [5] Dr. S. Raghavan, D. Sriram Kumar, M. S. Kishore Kumar, International Journal of Microwave and Optical Technology, 419 (2008).
- [6] K. P. Ray, S. Nikhil, A. Nair, International Journal of Microwave and Optical Technology, 205 (2009).
- [7] Amit A. Deshmukh, K. P. Ray, A. Mainkar, J. Gohil, P. Mahale, International Journal of Microwave and Optical Technology, 153 (2009).
- [8] Vidya Sagar chintakindi, Dr. Shyam Sundar Pattnaik, Dr. O. P. Bajpai, S. Devi, P. K. Patra, K. M. Bakwad, International Journal of Microwave and Optical Technology, 90 (2009).
- [9] K. L. Wong, W. H. Hsu, Electron. Letters, **33**, 2085 (1997).
- [10] X. Hao, J. Ma, D. Zhang, X. Xu, Y. Yang, H. Ma, S. Ai, Applied Physics A, **75**(7), 397 (2002).
- [11] S. Raghavan, T. Shanmuganantham, M. S. Kishore Kumar, Microwave and Optical Technology Letters, **50**, 2008.
- [12] K. F. Tong, K. M. Luk, K. F. Lee, R. Q. Lee, IEEE Trans. on Antennas Prop., **AP-48**(6), 954 (2000).
- [13] K. L. Wong, C. L. Tang, J. Y. Chiou, IEEE Trans. on Antennas and Propagation, **AP-50**(6), 827 (2002).
- [14] A. Porch, D. Morgan, R. Perks, M. Jones, P. P. Edwards, Journal of Applied Physics, **95**(9), (2004).
- [15] M. Abbaspour, H. R. Hassani, Progress In Electromagnetic Research Letters, **1**, 61 (2008).
- [16] H. Osman, E. A. Aballah, A. A. Abdel Rhim, PIERS Online, **4**(7), 761 (2008).
- [17] J. Ansari, R. B. Ram, Progress In Electromagnetic Research Letters, **4**, 17 (2008).
- [18] J. Ansari, P. Singh, S. K. Dubey, R. U. Khan, B. R. Vishwakarma, Microwave and Optical Technology Letters, **51**(2), 324 (2009).
- [19] G. Rafi, L. Shafai, IEE Proc. Microwave Antennas and Propagation, **151**, 435 (2004).
- [20] W. Chai, X. Zhang, J. Liu, PIERS Online, **3**(7), 1064 (2007).
- [21] S. Wi, Y.-S. Lee, J.-G. Yook, IEEE Transactions on Antennas and Propagation, **55**, 1196 (2008).
- [22] M. VanHest, M. Dabney, J. Perkins, D. Ginley, Applied Physics Letters, **87**(3), 345 (2005).
- [23] D. Caratelli, R. Cicchetti, G. Bit Babik, A. Faraone, IEEE Transactions on Antennas and Propagation, **54**, 1871 (2006).
- [24] G. Rafi, G. Z. and L. Shafai, Electronic Letters, **40**(19), 1166 (2004).
- [25] A. T. Silver, A. Sanchez-Juarez, A. Avila-Garcia, International Symposium on H-Fuel Cell Photovoltaic Systems **55**, 1 (1998).
- [26] D. P. Fromm, A. Sundaramurthy, P. J. Schuck, G. Kino, W. E. Moerner, Nano Lett. **4**(5), 957 (2004).
- [27] F. Kong, B. Wu, H. Chen, J. A. Kong, Opt. Express, **15**(19), 12331 (2007).

*Corresponding author: ahmed_733@yahoo.com